

# Conformational solution studies of the anti-microbial temporin A retro-analogues by using NMR spectroscopy

WOJCIECH KAMYSZ,<sup>a</sup> BEATA MICKIEWICZ,<sup>b</sup> KATARZYNA GREBER<sup>a</sup> and SYLWIA RODZIEWICZ-MOTOWIDŁO<sup>b\*</sup>

<sup>a</sup> Faculty of Pharmacy, Medical University of Gdańsk, Gdańsk, Poland

<sup>b</sup> Faculty of Chemistry, University of Gdańsk, Gdańsk, Poland

Received 8 January 2007; Accepted 13 January 2007

**Abstract:** Temporin A (TA) is a small, basic and highly hydrophobic peptide, isolated from the skin of the European red frog, *Rana temporaria*. The TA (FLPLIGRVLSGIL-NH<sub>2</sub>) displays a broad spectrum of anti-microbial activity against Gram-positive bacteria and fungi *Candida albicans*. In this study we investigate the solution structure of two TA retro-analogues, (6-1)(7-13)-TA (GILPLFRVLSGIL-NH<sub>2</sub>) and retro-TA (LIGSLVRGILPLF-NH<sub>2</sub>) by using nuclear magnetic resonance (NMR). The 3D solution structure of the analogues was established by using inter-proton distances and vicinal coupling constants in the *Simulated Annealing* (SA) calculations (XPLOR program). The NMR conformational studies show the existence of the helical structure in the middle part of the (6-1)(7-13)-TA peptide and an unordered structure of the retro-TA analogue under the D<sub>3</sub>-TFE/H<sub>2</sub>O (3:7, v/v) conditions. Our investigations have shown that the hydrophobic cluster at N-terminus with the Pro amino acid residue in position 3 or 4, the helical structure and the amphipathic character of the peptide are responsible for the anti-microbial activity of the TA analogues. Copyright © 2007 European Peptide Society and John Wiley & Sons, Ltd.

**Keywords:** temporin A; analogues; anti-microbial peptides; NMR; structure; TFE

## INTRODUCTION

The temporins (A–G, H, K and L) belong to the shortest anti-microbial peptides occurring in nature. They are composed of 10–13 amino acid residues. These peptides were isolated from the skin of the European red frog *Rana temporaria* [1]. They are active against both Gram-positive and Gram-negative bacteria and are found to be non-toxic to human red blood cells. The primary structure of the temporins is highly variable, but a majority of them contain a single basic residue (arginine or lysine). The common feature of all temporins is a free amino N-terminus and  $\alpha$ -amidation on C-terminus of the molecule [2–4].

It is thought that the anti-microbial mechanism of temporins is based on the leakage of water and ions through pores in the bacterial cell membrane [5]. Temporin A (TA) exerts its anti-microbial character either by the ability to form a transmembrane pore via a barrel-stave mechanism [6,7], or of a 'carpet' on the membrane surface via a 'carpet-like' model [8–11]. Nevertheless, the exact mechanism by which the temporins disturb the bacterial membrane is not known. Magnoni *et al.* [12] reported that the ability of temporins to destroy microbial cells is not dependent on membrane composition, since they lysed artificial vesicles built of zwitterionic and acid phospholipids, as well.

TA is the most well known among the temporins. It is a 13-amino acid (FLPLIGRVLSGIL-NH<sub>2</sub>) strongly hydrophobic and basic peptide, which exhibits anti-bacterial activity (mainly against Gram-positive cocci including methicillin-resistant *Staphylococcus aureus* and vancomycin-resistant *Enterococcus faecium*) and anti-fungal activity (yeast-like *Candida albicans*). The hydrophobic N-terminal residue, Arg7 and two Ile residues (5 and 12) are described as critical ones for anti-bacterial activity [13]. Substitution of the N-terminal Phe of TA for Lys resulted in a dramatic reduction of anti-bacterial activity [14]. However, anti-microbial efficacy does not stem from strict chiral interactions between particular amino acids and microbial membranes, because TA built of all-D enantiomers retains its lytic activity [15]. Interestingly, replacement of the isoleucine by leucine residues in positions 5 and 12 in native TA (TA L512) caused an increase in anti-microbial potency, but the replacement of Leu by Ala at the same positions abolished totally the bacteria killing activity [13]. However, the all-D enantiomer with Leu residues in positions 5 and 12 is cytotoxic [15]. The native TA, as well as its TA L512 analogue, did not show any toxic effect towards keratinocytes cultured *in vitro* at concentrations that are totally bactericidal, thus being promising molecules against multi-resistant bacterial infections [15].

This work describes the NMR conformational analysis of two retro-analogues (retro-TA (LIGSLVRGILPLF-NH<sub>2</sub>) and (6-1)(7-13)-TA (GILPLFRVLSGIL-NH<sub>2</sub>)). Until now, NMR investigations of the native TA in water and in 70% TFE have been reported [13]. The NMR results show

\*Correspondence to: S. Rodziewicz-Motowidło, Faculty of Chemistry, University of Gdańsk, Sobieskiego 18, 80-952 Gdańsk, Poland; e-mail: sylwia@chem.univ.gda.pl

that TA adopts a mainly random-coil structure in water and as  $\alpha$ -helical structure in the TFE solution, but the 3D structure of this peptide was only modelled, but not calculated under consideration of NMR constraints. The NMR studies of TA in a membrane mimetic environment (aqueous solution of DPC) and structural calculations show the peptide to possess a highly  $\alpha$ -helical structure [16]. According to our CD experiments [17], the retro-analogues of TA are mainly random coil at different pH in phosphate buffer solutions. In water, at a relatively low TFE concentration (30%) and in the presence of SDS micelles, the (6-1)(7-13)-TA peptide adopts mainly  $\alpha$ -helical structure, whereas the retro-TA assumes mostly unordered conformation under hydrophilic or hydrophobic conditions. This can explain the much lower anti-microbial activity of this analogue [17]. Knowledge of the 3D structure of the native TA peptide [13,16] and its active and inactive analogues could help in designing the new analogues. Such research usually leads to a better understanding of the structural features of a peptide that are important for assessing its antibiotic and/or toxic properties.

In our NMR investigations, the TFE solutions, which mimic the hydrophobic membrane environment quite well and may introduce  $\alpha$ -helical structures in the peptides were used. The biological membrane is much better mimicked by the presence of the SDS micelles. Nevertheless, the CD investigations show that

both analogues adopt identical structure in the TFE solutions and in the presence of the SDS micelles [17]. Therefore, in our NMR experiments, the TFE solvent was used.

## MATERIALS AND METHODS

### NMR Spectroscopy

The peptides were synthesized by the solid-phase technique and purified by reversed phase HPLC as described in the literature [17]. For NMR measurements, the peptide was dissolved in  $D_3$ -TFE/ $H_2O$  (3:7, v/v) solutions. The peptides concentration, 3 mM, was very low because at higher concentration the peptides begin to aggregate. All experiments were carried out on a Varian Unity 500 Plus spectrometer. All 2D NMR spectra were recorded at 30 °C except for the temperature coefficients of the chemical shifts, which were measured throughout the temperature range of 20–45 °C. The proton chemical shifts were referenced to the  $H_2O$  frequency measured with respect to the internal sodium 3-trimethylsilylpropionate (TSP). NMR data were processed using the Vnmr program [18] and analyzed using the XEASY software [19]. Sequential backbone resonance assignments were achieved in the following experiments: DQF-COSY [20]; TOCSY [21] with mixing times of 80 ms; NOESY [22] with a mixing time of 150 ms; ROESY [23] with a mixing time of 200 ms. All spectra were measured with water signal pre-saturation pulse. With the TOCSY (Figure 1) and DQF-COSY

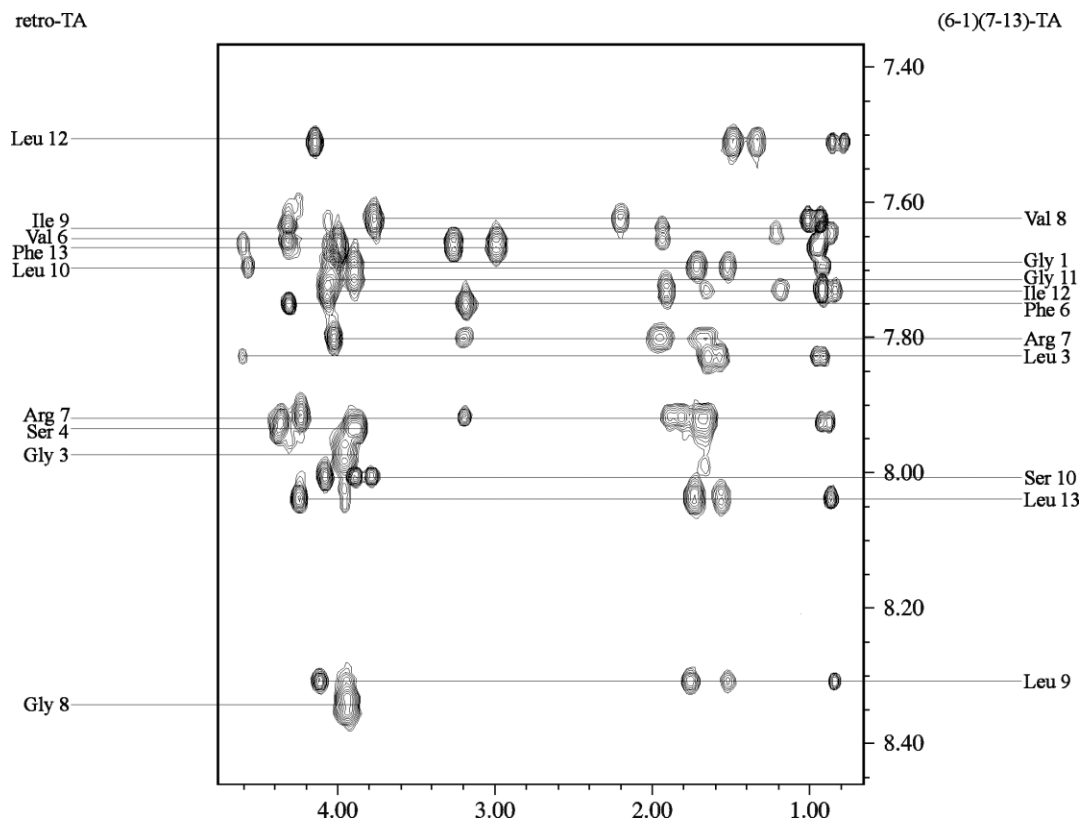


**Figure 1** The  $\alpha$ -amide region of a TOCSY spectrum (80 ms) at 30 °C of the retro-TA (on the left) and (6-1)(7-13)-TA (on the right) peptides in  $D_3$ -TFE/ $H_2O$  (3:7, v/v) solution.

spectra the proton chemical shifts were recognized (Tables 1 and 2) and using the ROESY spectrum the sequence of two analogues was confirmed.

The  $^3J_{\text{NH}\alpha}$  vicinal couplings constants were determined by 2D DQF-COSY experiments (Tables 1 and 2). The estimated experimental error was 0.3 Hz. The distance constraints and coupling constants were used in the HABAS program [24] of the DYANA package [25] to generate  $\phi$ ,  $\psi$ , and  $\chi^1$  dihedral angle constraints and stereospecific assignments. The dihedral angle constraints were calculated from the Karplus equation [24] with A = 6.4, B = -1.4 and C = 1.9 parameters [26].

The rotating frame nuclear Overhauser effect (ROE) intensities were determined from the ROESY spectrum of the TA analogues. The ROE volumes were integrated and calibrated with the XEASY software [19]. The ROE integrated volumes showed an error below 2%. After internal calibration, the cross-peaks obtained from the ROESY experiment were converted into upper distance limits by the CALIBA program of the DYANA package [25].

### The Structure Calculations

The structures of the retro-TA and (6-1)(7-13)-TA peptides were determined using the XPLOR software, Version 3.1 [27]. The structure of each peptide was produced using distance and torsion angle restraints. The distance restraints were calculated based on the ROE intensities, which were picked up on the ROESY spectrum. The ROE volumes were integrated and calibrated with the XEASY [19] software. Because of the spectral overlap, only well-separated cross-peaks were integrated and further used in the structure calculations. For XPLOR 3D structure calculations the ROESY experiments provided for retro-TA 125 distance restraints and for (6-1)(7-13)-TA 110 restraints. For retro-TA, the restraint set contained 101 intra-residue and 24 ( $i, i + 1$ ); for (6-1)(7-13)-TA the restraint set constrained 76 intra-residue, 28 ( $i, i + 1$ ), 2

( $i, i + 2$ ) and 4 ( $i, i + 3$ ) ROEs. For retro-TA and for (6-1)(7-13)-TA, the HABAS program provided 26 and 27 torsion angles, respectively.

The structures of both peptides were calculated with the standard modules of the XPLOR program [27]. The calculations were carried using the CHARMM force field [28] *in vacuo* starting from a random structure. SA algorithm was used for both peptides. Electrostatic interactions and energy of hydrogen bonds were not directly included and *van der Waals* interactions were described with the simplified potential function. According to the NMR data, the inter-proton distances ( $f = 50 \text{ kcal/mol} \times \text{\AA}^2$ ), torsion angles ( $f = 5 \text{ kcal/mol} \times \text{rad}^2$ ) and geometry of the peptide group (all *trans*) ( $f = 500 \text{ kcal/mol} \times \text{rad}^2$ ) were kept fixed. Also, the chirality of all  $\text{C}^\alpha$  atoms, except for glycine residues, was fixed at L ( $f = 500 \text{ kcal/mol} \times \text{rad}^2$ ). For both molecules 300 cycles of SA were carried out. Each cycle included 27 000 iterations of 80 ps with the 3 fs steps. The molecule was maintained at 1000 K for 50 ps and annealed at 100 K for 29 ps. In the last 200 iterations (1 ps), energy minimization with the use of the Powell's algorithm [29] was performed. During SA refinement, the molecule was slowly cooled from 1000 to 100 K over 30 ps. Finally, 300 energy-minimized conformations were obtained. The set of the final conformations was clustered using the MOLMOL program [30].

The RMSD between heavy atoms at optimum superposition was taken as a measure of the distance between conformations, and the cut-off value of 4 Å was used to separate the families. In further analysis, five families of conformations for retro-TA and four families of conformations for (6-1)(7-13)-TA were considered. Molecular structures were drawn and analysed with the graphic MOLMOL program [30]. This program was also used to demonstrate the flexibility of the peptide structure and to display the electrostatic potential on the *van der Waals* surface.

**Table 1** Proton chemical shifts [ppm],  $^3J_{\text{HN}\alpha}$  vicinal coupling constants [Hz] and temperature coefficients of amide protons ( $\Delta\delta/\Delta T$ ) of the (6-1)(7-13)-TA in  $\text{D}_3\text{-TFE}/\text{H}_2\text{O}$  (3:7, v/v) solutions at 30 °C

Residue	Chemical shifts [ppm]					$^3J_{\text{HN}\alpha}$ [Hz]	$-\Delta\delta/\Delta T \times 10^{-3}$ [ppm/K]
	HN	H $\alpha$	H $\beta$	H $\gamma$	Others		
Gly1	7.689	4.021; 3.892	—	—	—	6.5	n
Ile2	8.163	4.318	1.850	1.476; 1.195	H $\delta$ 0.932; 0.871	d	6.6
Leu3	7.831	4.597	1.649	1.579	H $\delta$ 0.963; 0.913	d	6.9
Pro4	—	4.357	2.293; 2.060	1.905	H $\delta$ 3.909; 3.640	—	—
Leu5	7.301	4.073	1.648	1.553	H $\delta$ 0.906; 0.841	4.3	0.3
Phe6	7.753	4.304	3.183	—	H $\epsilon$ 7.310; H $\zeta$ 7.153 H $\delta$ 7.200	6.5	2.5
Arg7	7.801	4.027	1.945; 1.738	1.648	H $\delta$ 3.191; H $\epsilon$ 7.227	6.4	5.5
Val8	7.628	3.764	2.208	1.017; 0.941	—	7.6	3.8
Leu9	8.307	4.100	1.767	1.527	H $\delta$ 0.851	6.4	8.0
Ser10	8.008	4.077	3.888; 3.778	—	—	4.3	d
Gly11	7.706	4.063	—	—	—	d	0.2
Ile12	7.724	4.054	1.918	1.664; 1.197	H $\delta$ 0.928; 0.845	7.6	2.2
Leu13	8.038	4.236	1.735	1.566	H $\delta$ 0.874	6.5	5.0
NH <sub>2</sub> 14	7.060; 6.862	—	—	—	—	—	—

n, not found; d, difficult to measure.

**Table 2** Proton chemical shifts [ppm],  $^3J_{\text{HN}\alpha}$  vicinal coupling constants [Hz] and temperature coefficients of amide protons ( $\Delta\delta/\Delta T$ ) of the retro-TA in  $D_3$ -TFE/ $H_2O$  (3:7, v/v) solutions at 30 °C

Residue	Chemical shifts [ppm]					$^3J_{\text{HN}\alpha}$ [Hz]	$-\Delta\delta/\Delta T \times 10^{-3}$ [ppm/K]
	HN	H $\alpha$	H $\beta$	H $\gamma$	Others		
Leu1	7.922	4.224	1.660	1.648	H $\delta$ 0.957; 0.895	6.438	n
Ile2	7.599	4.236	1.906	1.558; 1.236	H $\delta$ 0.967; 0.906	d	0.2
Gly3	7.973	3.947	—	—	—	6.470	2.1
Ser4	7.931	4.363	3.886	—	—	6.474	3.1
Leu5	7.987	4.350	1.666	1.652	H $\delta$ 0.947; 0.871	d	d
Val6	7.666	3.991	2.123	0.952; 0.874	—	6.737	3.7
Arg7	7.917	4.228	1.890; 1.817	1.677	H $\delta$ 3.190; H $\epsilon$ 7.172	6.459	—
Gly8	8.345	2.932	—	—	—	5.869	7.1
Ile9	7.637	4.306	1.940	1.499; 1.220	H $\delta$ 0.915; 0.855	8.628	5.8
Leu10	7.698	4.563	1.722	1.527	H $\delta$ 0.925	6.513	4.7
Pro11	—	4.391	2.208; 1.991	1.837	H $\delta$ 3.793; 3.519	—	—
Leu12	7.513	4.132	1.492	1.338	H $\delta$ 0.860; 0.786	8.481	0.07
Phe13	7.672	4.597	3.261; 2.992	—	H $\delta$ 7.273; H $\zeta$ 7.215 H $\epsilon$ 7.245	10.762	3.8
NH <sub>2</sub> 14	6.904; 6.770	—	—	—	—	—	5.7

n, not found; d, difficult to measure.

## RESULTS

### NMR Experiments

In this work, an NMR conformational study of two TA analogues of (6-1)(7-13)-TA (GILPLFRVLSGIL-NH<sub>2</sub>) and retro-TA (LIGSLVRGILPLF-NH<sub>2</sub>) in  $D_3$ -TFE/ $H_2O$  (3:7, v/v) is presented. Inspection of the NMR spectra revealed that the peptide bonds of both peptides exist as stable *trans*-isomers. In the ROESY spectra of both peptides, no exchange ROE cross-peaks were observed. Although the amino acid composition of both peptides is the same, the chemical shifts of the same amino acids are different in the TOCSY spectra of the studied peptides (Figure 1). Because the chemical shifts are a very sensitive indicator of the secondary structure of peptides and proteins [31], the different chemical shifts in NMR spectra of the both peptides predict completely different 3D structures.

Figure 2(a) and (b) summarizes the ROE patterns, the values of vicinal coupling constants  $^3J_{\text{HN}\alpha}$  and the temperature coefficients ( $\Delta\delta/\Delta T$ ) obtained for the peptides. In the case of the (6-1)(7-13)-TA analogue, the strong H $^\alpha$ (i)-H $^N$ (i+1) ROEs and weak H $^\alpha$ (i)-H $^N$ (i,i+3) and H $^\alpha$ (i)-H $^\beta$ (i,i+3) ROEs indicate an  $\alpha$ -helical fragment in the Phe6-Ser10 region. Additionally, the strong cross-peaks H $^\alpha$ (i)-H $^N$ (i+1) and H $^\beta$ (i)-H $^N$ (i+1) in the Val8-Gly11 fragment suggest the formation of  $\beta$ -turns in the C-terminal part of the peptide. However, only two amino acids, Leu5 and Ser10, have small ( $\sim 4$  Hz)  $^3J_{\text{HN}\alpha}$  vicinal coupling constants, characteristic of the  $\alpha$ -helical structure. The  $^3J_{\text{HN}\alpha}$  vicinal coupling constants ( $>6$  Hz) for the remaining

amino acids do not confirm the presence of the stable  $\alpha$ -helical structure of the whole (6-1)(7-13)-TA peptide. These suggest that under experimental conditions, the  $\alpha$ -helical conformation is only the local state in the conformational equilibrium of this peptide. Temperature coefficients, higher than  $-3.0 \times 10^{-3}$  (Table 1), of the Leu5, Phe6, Gly11 and Ile12 amide protons indicate the very strong hydrogen bond formation of these amide protons, which could stabilize the  $\alpha$ -helical structure.

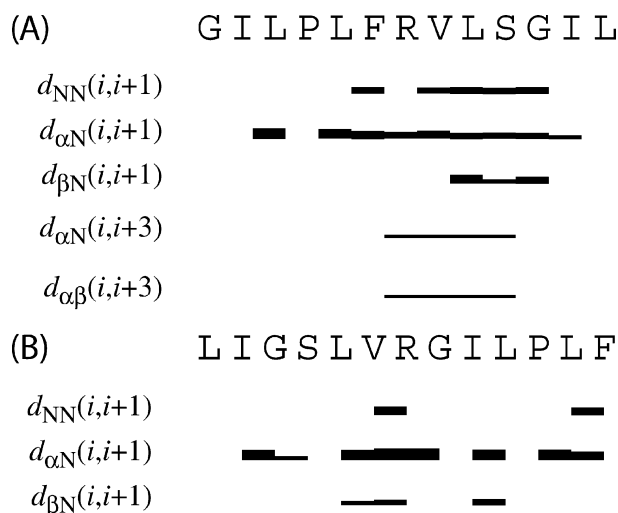


**Figure 2** Summary of ROE connectivities of (A) (6-1)(7-13)-TA and (B) retro-TA peptides, measured in ROESY spectrum (200 ms) at 30 °C in  $D_3$ -TFE/ $H_2O$  (3:7, v/v) solution. The height of the bars reflects the strength of the ROE correlation as strong, medium or weak.

With the retro-TA peptide, no characteristic ROE pattern was found. Although the solvent, which may introduce  $\alpha$ -helical structures in peptides, was used, the  $\alpha$ -helical structure was not found in the case of the retro-TA. The presence of the  $H^\alpha(i)-H^N(i+1)$  and  $H^\beta(i)-H^N(i+1)$  ROE cross-peaks suggests that the  $\beta$ -turns at positions 5,6; 6,7 and 9,10 are populated (the  $i$  and  $i+1$  positions of the  $\beta$ -turn are shown in Figure 2). Also, large  $^3J_{HN\alpha}$  vicinal coupling constants ( $\sim 6.5$  Hz) and low values of the temperature coefficients of the amide protons (except for Ile2 and Leu12, refer Table 2) confirm the lack of the characteristic structure of this peptide.

### The Calculated Structures

In the case of the (6-1)(7-13)-TA analogue, the peptide adopts a mainly  $\alpha$ -helical structure in the middle part of the structure (Arg7-Gly11) (Figure 3). The  $N$ -terminal part of the peptide forms a stable type  $\beta$ -turn in the Leu3-Phe6 region. This  $\beta$ -turn is stabilized by a strong  $6 \rightarrow 4$  hydrogen bond. The formation of this  $\beta$ -turn allows to form a bend structure on the  $N$ -terminus with the strong hydrophobic interactions between side chains of the Ile2 and Leu3, Ile2 and Phe6 amino acids. The  $C$ -terminal part of the peptide (Gly11-Leu13) is mostly unordered. It is very interesting that the positively charged Arg7 side-chain is strongly exposed to the solvent, where it may act as an 'electrostatical pin' between the peptide and the negatively charged bacterial membrane. Formation of the helical structure allows the (6-1)(7-13)-TA to exist as a very amphiphatic molecule, where the Arg8 and Ser10 create hydrophilic part of the molecule and the rest of the hydrophobic amino acids form a hydrophobic core on the opposite side of the molecule. The RMSD value of all the  $C^\alpha$  atoms is 1.94 Å, whereas that of the  $C^\alpha$  atoms from the helical region is very low (0.36 Å). In all calculated

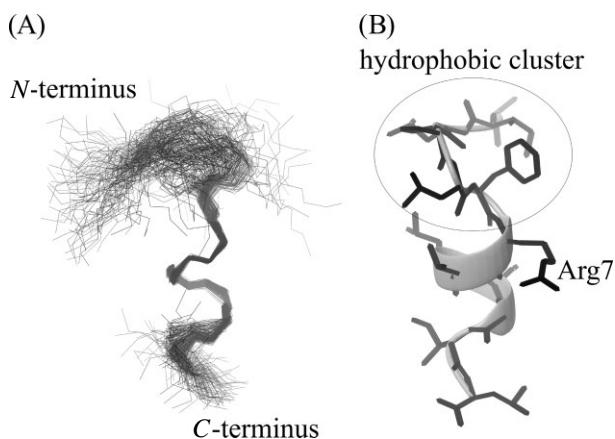


**Figure 3** (A) The superposition of backbone atoms of the amino acid residues Arg7 to Gly11 of the (6-1)(7-13)-TA peptide. (B) The helical structure with marked hydrophobic cluster and hydrophilic Arg7 amino acid residue.

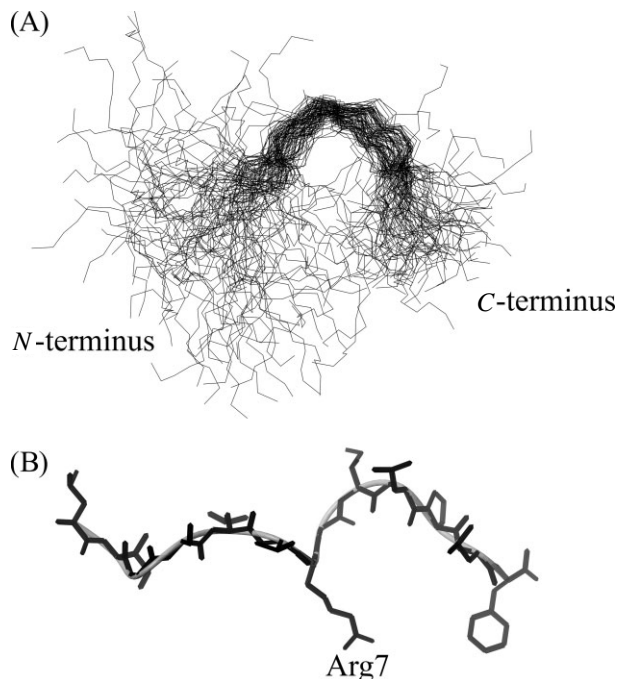


**Figure 4** (A) The superposition of backbone atoms of amino acid residues from Arg7 to Pro11 of retro-TA peptide. (B) One of the calculated structures with marked side chains.

structures the  $6 \rightarrow 4$ ,  $11 \rightarrow 7$  and  $12 \rightarrow 8$  hydrogen bonds in the main chain are formed. The formation of all these hydrogen bonds is in very good agreement with the experimental NMR data of  $\Delta\delta/\Delta T$  values.

As the CD experiments have shown [17], the structure of the retro-TA peptide is mainly unordered. Our structures, calculated on the basis of the NMR data (Figure 4), also show that this peptide forms an unordered structure with flexible  $N$ - and  $C$ -terminus. In all the calculated structures, only one  $13 \rightarrow 11$  hydrogen bond in the main chain is created. Also, no characteristic amphiphatic sides were found in the retro-TA peptide. In this peptide, the hydrophobic amino acids do not form a characteristic hydrophobic core. The hydrophobic amino acids form two separate fragments of the hydrophobic centres on the  $N$ - (Leu1, Ile2, Leu5 and Val6) and  $C$ -terminus (Ile9, Leu10, Leu12 and Phe13), which are separated by the polar Arg7 amino acid residue. The RMSD value of all the  $C^\alpha$  atoms is 3.89 Å, and is much higher than that in the (6-1)(7-13)-TA analogue.

### DISCUSSION

Wade *et al.* (2000), who studied 18 analogues of TA and its analogues, concluded that the helicity of a peptide can be one of the critical parameters for anti-bacterial character [13]. Our NMR experiments and the structure calculations confirm this hypothesis. The partially helical and amphiphatic features are

responsible for the high anti-microbial activity of the (6-1)(7-13)-TA analogue, whereas the unordered structure of the retro-TA analogue is responsible for the much lower anti-microbial activity.

Although the amino acid composition of TA and its retro-analogues is the same, the amino acids sequences, 3D structures and biological activities are different. Such properties of Phe1, Arg7 and two Ile residues (5 and 12) were reported as critical ones for anti-bacterial activity of TA [13] owing to the formation of amphipathic structure. In all the three sequences (TA, (6-1)(7-13)-TA and retro-TA), some of these characteristic features are observed. In these three peptides, the basic amino acid, Arg, is in the same 7th position; in the important 5th and 12th positions are the hydrophobic amino acids, and the C-terminus is occupied by the amide group. At the first position in the active TA and the much less active retro-TA, the strongly hydrophobic amino acid is found, whereas in the active (6-1)(7-13)-TA analogue, the sequence starts from the slightly hydrophobic Gly amino acid. With (6-1)(7-13)-TA, the N-terminal fragment is mostly hydrophobic as in native TA, whereas the retro-TA contains the hydrophilic Ser4 amino acid in the N-terminal sequence and disrupts the hydrophobic cluster formation. Therefore, in our opinion, a strongly hydrophobic amino acid in position 1 is not required for anti-microbial activity. Probably, all the hydrophobic amino acids at the N-terminus of TA and its active analogues are responsible for the biological activity of these peptides. The hydrophobic amino acids at the N-terminus can form a hydrophobic cluster, thus allowing to interact with biological membrane. Therefore, the substitution of the N-terminal hydrophobic Phe of TA for hydrophilic Lys resulted in the dramatic reduction of hydrophobicity and anti-bacterial activity [13]. The hydrophobic cluster formation at the N-terminus in active peptides is possible due to the Pro residue, which allows TA to form the bent structure. The Ser and Pro amino acids in the active TA and (6-1)(7-13)-TA are at the same or similar position, whereas in the case of the much less active retro-TA, the Ser and Pro amino acids occupy the 4th and 11th positions, respectively.

The stable  $\alpha$ -helical structure formation in the 7-11 fragment of the (6-1)(7-13)-TA analogue is in very good agreement with the results obtained by D'Abramo *et al.* [32], who found that for  $\alpha$ -helix formation of TA, the most energetically accessible region is the one extending from the 7th to the 10th amino acid residue.

Bearing all this in mind, it is concluded that the anti-microbial activity of TA and its analogues is not necessarily related to the amino acid composition, but to the structural features such as the hydrophobic cluster at the N-terminus with the Pro amino acid residue at positions 3 or 4, the helical structure and the amphipathic character of the peptide structure.

## Acknowledgements

This work was supported by University of Gdańsk, Grant BW/8000-5-0280-5. W. Kamysz is a holder of the scholarship of the Foundation for Polish Science. B. Mickiewicz is supported by a EFS project ZPORR/2.22/II/2.6/ARP/U/2/05. The calculations were carried out in the TASK in Gdańsk, Poland.

## REFERENCES

1. Simmaco M, Mignogna G, Canofeni S, Miele R, Mangoni ML, Barra D. Temporins, antimicrobial peptides from the European red frog *Rana temporaria*. *Eur. J. Biochem.* 1996; **242**: 788-792.
2. Conlon JM, Kolodziejek J, Nowotny N. Antimicrobial peptides from ranid frogs: taxonomic and phylogenetic markers and a potential source of new therapeutic agents. *Biochem. Biophys. Acta* 2004; **1696**: 1-14.
3. Mangoni ML, Rinaldi AC, Giulio AD, Mignogna G, Bozzi A, Barra D. Structure-function relationships of temporins, small antimicrobial peptides from amphibian skin. *Eur. J. Biochem.* 2000; **267**: 1447-1454.
4. Simmaco M, Mignogna G, Canofeni S, Miele R, Mangoni ML, Barra D. Temporins, antimicrobial peptides from the European red frog *Rana temporaria*. *Eur. J. Biochem.* 1996; **242**: 788-792.
5. Rinaldi AC, Mangoni ML, Rufo A, Luzi C, Barra D, Zhao H. Temporin L: antimicrobial, haemolytic and cytotoxic activities, and effects on membrane permeabilization in lipid vesicles. *Biochem. J.* 2002; **368**: 91-100.
6. Oren Z, Shai Y. Mode of action of linear amphipathic  $\alpha$ -helical antimicrobial peptides. *Biopolymers* 1998; **47**: 451-463.
7. Rapaport D, Shai Y. Interaction of fluorescently labeled pardaxin and its analogues with lipid bilayers. *J. Biol. Chem.* 1991; **266**: 23769-23775.
8. Zasloff M. Antimicrobial peptides of multicellular organism. *Nature* 2002; **415**: 389-395.
9. Ludtke SJ, He K, Harroun TA, Yang L, Huang HW. Membrane pores induced by magainin. *Biochemistry* 1996; **35**: 13723-13728.
10. Matsuzaki K, Biochim M. Why and how are peptide-lipid interactions utilized for self-defence? Magainins and tachyplesins as archetypes. *Biochem. Biophys. Acta-Biomem.* 1999; **1462**: 1-10.
11. Pouny Y, Rapaport D, Mor A, Nicolas P, Shai Y. Interactions of antimicrobial dermaseptin and its fluorescently labeled analogs with phospholipid-membranes. *Biochemistry* 1992; **31**: 12416-12423.
12. Mangoni ML, Rinaldi AC, Di Giulio A, Mignogna G, Bozzi A, Barra D, Simmaco M. Structure-function relationships of temporins, small antimicrobial peptides from amphibian skin. *Eur. J. Biochem.* 2000; **267**: 1447-1454.
13. Wade D, Silberring J, Soliymani R, Heikkinen S, Kilpelainen I, Lankinen H, Kuusela P. Antibacterial activities of temporin A analogues. *FEBS Lett.* 2000; **479**: 6-9.
14. Andreu D, Rivas L. Antimicrobial peptides. *Biopolymers* 1998; **47**: 415-433.
15. Mäntylä T, Sirola H, Kansanen E, Korjamo T, Lankinen H, Lappalainen K, Välimaa AL, Harvima I, Närviänen A. Effect of temporin A modifications on its cytotoxicity and antimicrobial activity. *APMIS* 2005; **113**: 497-505.
16. Auriemma L, Carotenuto M, Mazella di Bosco A, Mangowi ML, Campiglia P, Grieco P. Conformational behaviour of temporin A and temporin L by NMR spectroscopy in different environmental conditions. *J. Pept. Sci.* 2006; **12**(Suppl. S): 192.
17. Kamysz W, Mickiewicz B, Rodziewicz-Motowidło S, Greber K, Okrój M. Conformational behaviour of temporin A and temporin L by NMR spectroscopy in different environmental conditions. *J. Pept. Sci.* 2006; **12**: 533-537.

18. Varian, nuclear magnetic resonance instruments, VnmrTM Software, Revision 5.3B 1/97.
19. Bartles C, Xia T, Billeter M, Günter P, Wüthrich K. The program XEASY for computer-supported NMR spectral-analysis of biological macromolecules. *J. Biomol. NMR* 1995; **5**: 1–10.
20. Piantini U, Sorrensen OW, Ernst RR. Multiple quantum filters for elucidating NMR coupling networks. *J. Am. Chem. Soc.* 1982; **104**: 6800–6810.
21. Bax A, Davis DG. MLEV-17-based two-dimensional homonuclear magnetization transfer spectroscopy. *J. Magn. Reson.* 1985; **65**: 355–360.
22. Jeener J, Meier BH, Bachmann P, Ernst RR. Investigation of exchange processes by 2-dimensional NMR-spectroscopy. *J. Chem. Phys.* 1979; **71**: 4546–4553.
23. Bax A, Davis DG. Practical aspects of two-dimensional transverse NOE spectroscopy. *J. Magn. Reson.* 1985; **63**: 207–213.
24. Karplus M. Contact electron-spin coupling of nuclear magnetic moments. *J. Chem. Phys.* 1959; **30**: 11–15.
25. Güntert P, Braun W, Wüthrich K. Efficient computation of 3-dimensional protein structures in solution from nuclear-magnetic-resonance data using the program DIANA and the supporting programs CALIBA, HABAS and GLOMSA. *J. Mol. Biol.* 1991; **217**: 517–530.
26. Pardi A, Billeter M, Wüthrich K. Calibration of the angular-dependence of the amide proton-C-alpha proton coupling-constants,  $^3J_{\text{HN}\alpha}$ , in a globular protein—use of  $^3J_{\text{HN}\alpha}$  for identification of helical secondary structure. *J. Mol. Biol.* 1984; **180**: 741–751.
27. Brünger AT. *The X-PLOR Software Manual. Version 3.1.* Yale University Press: New Haven, CT, 1992.
28. Brooks BR, Bruccoleri RE, Olafson BD, States DJ, Swaminathan S, Karplus M. CHARMM: a program for macromolecular energy, minimization, and dynamics calculations. *J. Comput. Chem.* 1983; **4**: 187–217.
29. Powell MJD. Restart procedures for conjugate gradient method. *Math. Prog.* 1977; **12**: 241–254.
30. Koradi R, Billeter M, Wüthrich K. MOLMOL: a program for display and analysis of macromolecular structures. *J. Mol. Graph.* 1996; **15**: 51.
31. Wishart DS, Sykes BD, Richards FM. The chemical-shift index—a fast and simple method for the assignment of protein secondary structure through NMR-spectroscopy. *Biochemistry* 1992; **31**: 1647–1651.
32. D'Abramo D, Rinaldi AC, Bozzi A, Amadei A, Mignogna G, Di Nola A, Aschi M. Conformational behaviour of Temporin A and Temporin L in aqueous solution: a computational/experimental study. *Biopolymers* 2006; **81**: 215–224.